■ **Supramolecular Chemistry** │*Hot Paper*│

Dual Visible Light-Triggered Photoswitch of a Diarylethene Supramolecular Assembly with Cucurbit[8]uril

Guoxing Liu,[a] Ying-Ming Zhang,[a] Conghui Wang,[a] and Yu Liu*[a, b]

Abstract: Research on photochromic molecules switched by visible light is of particular interest for their application in bioimaging and stimuli-responsive materials. Here, a photoswitchable supramolecular assembly comprised of monocharged bispyridinium-modified diarylethenes (DAEs) and cucurbit[8]uril (CB[8]) has been constructed, which exhibits reversible photochromic behaviour with visible light in both directions. The transformation of CB[8] not only prompts the DAEs to form charge-transfer complexes, but also restricts its intramolecular rotation to enhance fluorescence emission. In this CB[8]-containing supramolecular system, the π-conjugation is extended and its absorption is bathochromically shifted for visible light-driven cyclization of DAEs. Meanwhile, the fluorescence of the supramolecular assembly can also be reversibly modulated by visible light. These findings may furnish a new strategy for the development of visible light-driven fluorescent biomaterials and molecular machines.

Molecular switches based on photoactive building blocks, such as spiropyran, azobenzene, and diarylethene, have attracted wide attention for their inventive application in constructing molecular machines,[1] self-healing materials,[2] optical memory storage devices,[3] photocontrolled photodynamic therapy systems,[4] and optically switchable electronic devices.[5] Among these photosensitive molecules, diarylethenes (DAEs) are one of the most attractive molecules due to their excellent thermal stability, rapid response and fatigue resistance.[6] Usually, at least one direction in the conversion between two optical isomers of DAEs should be triggered by ultraviolet (UV) light, which severely hampers their application in biological fields because of the serious shortcomings of UV light, including low transparency, nonselective absorption, and damages to cells and tissues.[7] Therefore, it is highly imperative to develop visible light-triggered DAE-based photochromic derivatives in

both directions. To achieve this goal, several strategies mainly through covalently chemical modification have been explored, such as extended π-electron conjugation,[8] triplet–triplet energy transfer,[9] energy up-conversion,[10] multiphoton absorption[11] and electron transfer.[12] However, noncovalent supramolecular approach to achieve this function has not been implemented, to the best of our knowledge. Herein, we utilized supramolecular approach to realize the photoreaction of DAEs in both directions upon visible light irradiation.

On the other hand, cucurbit[*n*]urils, an important class of macrocyclic hosts, can self-assemble with organic cations as guests to form stable host–guest complexes.[13] Among which, cucurbit[8]uril (CB[8]), possessing a larger cavity, readily forms charge-transfer (CT) complexes with guest molecules in a 1:2 molecular ratio, and has been extensively employed to construct various topological nanoarchitectures,[14] stimuli-responsive molecular machines,[15] and tunable photoluminescence materials.[16] Therefore, in this work, combining the photochromic property of DAEs with the noncovalent binding of CB[8], we synthesized the DAE-bridged monocharged bispyridinium salts **1** and **2** with *para-* and *meta*-substitution (Scheme 1), which were well-defined as the fluorescent molecular rotors with electron-donor (phenylthiophene) and acceptor (bispyridinium) moieties. The rational integration of the DAE derivatives with CB[8] was expected to enhance the π-conjugation of a self-assembled nanosystem through a complexation-induced intermolecular CT interaction, thus resulting in the bathochromic shift of the absorption band from UV to visible region and more importantly, endowing this system with the visible light-induced photocyclization ability. Meanwhile, the intramolecular rotation of single chemical bonds in **1** or **2** would be restricted for fluorescence emission upon complexation with CB[8]. This intriguing visible light-activated fluorescent supramolecular photoswitch is presented as described below.

The synthetic routes of photoswitchable molecules **1** and **2** were shown in Scheme S1 and comprehensively characterized (Figures S1–S11). Subsequently, their UV/Vis absorption spectra were investigated. Comparatively, an extra absorption maximum at 354 nm emerged in the open-form of **1** (OF-**1**), which could be assigned to the intramolecular CT interaction between electron-rich phenylthiophene and electron-deficient bispyridinium moieties (Figure S12a and Table S1). However, this phenomenon was inconspicuously presented in OF-**2**, which probably resulted from the diverse electron distribution caused by the different substitution position (Figure S12d and Table S1).

[a] G. Liu, Dr. Y.-M. Zhang, C. Wang, Prof. Dr. Y. Liu
College of Chemistry, State Key Laboratory of
Elemento-Organic Chemistry, Nankai University, Tianjin 300071 (P. R. China)
E-mail: yuliu@nankai.edu.cn

[b] Prof. Dr. Y. Liu
Collaborative Innovation Center of Chemical Science and
Engineering, Nankai University, Tianjin 300071 (P. R. China)

Supporting information and the ORCID identification number for the
author of this article can be found under https://doi.org/10.1002/
chem.201703562.
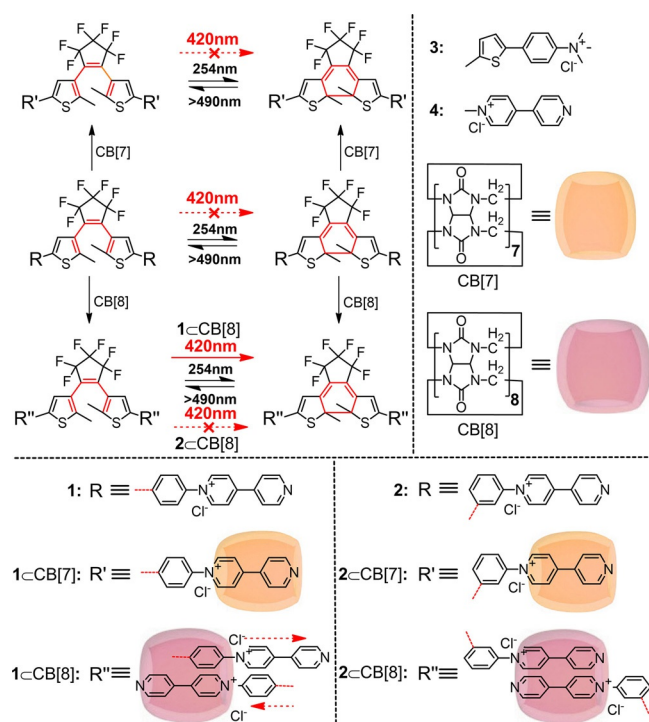
Scheme 1. Chemical structures of the employed guests, hosts, binary assemblies and their photochromic mechanism.

Figure 1. a) UV/Vis absorption, and b) fluorescence emission spectra of OF-**1** upon continuous addition of CB[8] in aqueous solution ([**1**] $= 1 \times 10^{-5}$ M; [CB[8]] $= 0$–1×10^{-5} M, excitation at 420 nm; slit $= 10, 10$). Inset: the spectral changes versus the molecular ratio of CB[8]/[OF-**1**].

Next, the molecular-assembling behaviour of photochromic molecular rotor **1** with CB[8] was investigated. As displayed in Figure 1 a, the absorption maximum of OF-**1** exhibited apparent bathochromic shift by 7 nm (from 274 to 281 nm) and 42 nm (from 354 to 396 nm) upon continuous addition of equivalent CB[8], which probably originated from the intermolecular CT interaction to enhance the degree of π-electron conjugation. Moreover, when excess CB[8] was added, the absorbance of OF-**1**⊂CB[8] no longer increased at 396 nm, implying that the optimal host–guest binding stoichiometry was in 1:1 molecular ratio. Additionally, the colourless solution became deep yellow, which further certificated the formation of CT complex in OF-**1**⊂CB[8] (Figure 1 a, inset). To further confirm our viewpoint, two fragments of OF-**1**, thiophene-involved trimethylammonium **3** and monocharged bispyridinium **4** were selected as references to further prove the molecular binding mode with CB[8]. As shown in Figure S17 a, and b, all the proton signals of **3** displayed a clear upfield shift, indicating two reference molecules were concurrently located in the cavity of CB[8] to form **3**₂⊂CB[8] complex. The binding stoichiometry of **3** with CB[8] was further verified by a Job plot, where a maximum peak at a molar ratio of 0.67 was observed, indicating a 1:2 host–guest binding stoichiometry (Figure S18). Similar ¹H NMR chemical shift phenomena were also presented in the **4**₂⊂CB[8] complex (Figure S17 d, and e).[13] However, when an equivalent amount of **3**, **4**, and CB[8] were mixed, a new ternary complex of **3**–**4**⊂CB[8] was formed in solution, which was further confirmed by a ROSEY spectrum (Figure S17 c and S19). These results show that the binding strength of CB[8] with equivalent **3** and **4** was much higher
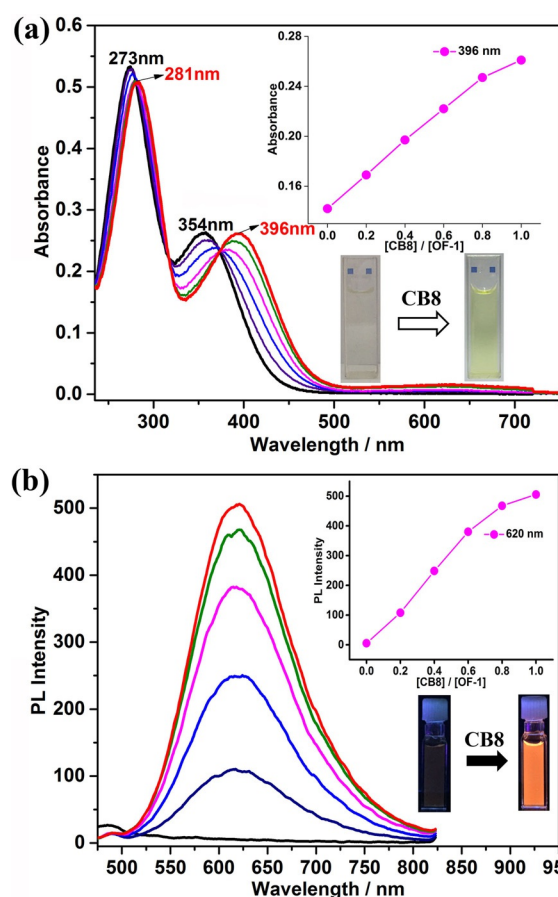
than that with individual **3** or **4**, because electron-rich **3**, electron-deficient **4** and CB[8] could self-assemble to a more stable ternary CT complex. More powerful proof came from the UV/Vis absorption spectral analysis. As displayed in Figure S20, a new long-wavelength absorption at 396 nm corresponding to the intermolecular CT interaction was observed, which was consistent with the UV/Vis absorption in the OF-**1**⊂CB[8] assembly (Figure 1 a). Overall, the aforementioned evidence doubtlessly uncovered the host–guest complexation in OF-**1**⊂CB[8] and the strong intermolecular CT interaction responsible for the UV/Vis absorption spectral change. Subsequently, the molecular assembly mode and morphology of **1** with CB[8] was investigated. The ¹H NMR titration of OF-**1** and OF-**1**⊂CB[8] showed that all the proton signals assigned to OF-**1** underwent an obvious upfield shift and showed a broadened pattern upon addition of CB[8], indicating the formation of OF-**1**⊂CB[8] assembly as a polymeric structure (Figure S14). Besides, no obvious change was observed in the presence of excess CB[8], which also indicated that the *n:n* OF-**1**⊂CB[8] linear assembly was the predominant species in solution. This binding stoichiometry of **1** with CB[8] was further verified by Job plot, in which a maximum peak at a molar ratio of 0.5 was observed (Figure S15). Furthermore, the intuitional proof came

from microscopic and dynamic light scattering (DLS) investigations. As shown in the TEM image, many nanofibers were found with an average width of 6.5 nm, indicating a possible secondary aggregation of several linear OF-1⊂CB[8] assemblies. The fibrous structure was also confirmed by SEM image (Figure 2 a and b). Furthermore, the hydrodynamic diameter of OF-1⊂CB[8] was detected as about 123.5 nm, here again corroborating the formation of large-sized nanoaggregate in solution (Figure S16). Based on these information, a reasonable assembling mode of linear nanoarchitecture 1⊂CB[8] was proposed, as illustrated in Figure 2 c. In the OF-1⊂CB[8] assembly, CB[8] was dynamically slipping along an axis comprised of two antiparallel monocharged bispyridinium moieties, leading to the extension of π-conjugation in the resultant linear supramolecular assembly.
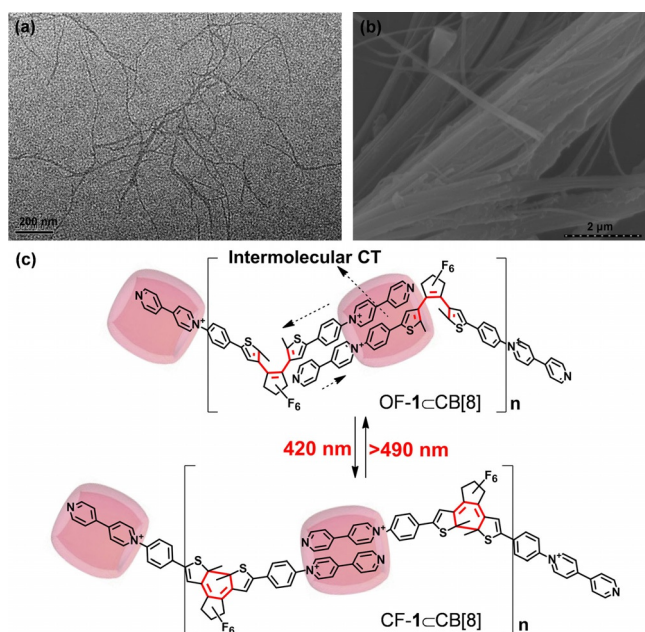

Figure 2. a) TEM, and b) SEM images of OF-1⊂CB[8] assembly; c) visible light-triggered photoisomerization mechanism of OF-1⊂CB[8] assembly.

More interestingly, there was a CB[8]-induced enhancement of fluorescence emission behaviours in the OF-1⊂CB[8] assembly; that is, strong orange–red fluorescence of OF-1 was observed at 620 nm by a factor of 65 in the presence of CB[8] (Figure 1 b). Accordingly, the fluorescence lifetime and quantum yield of the assembly OF-1⊂CB[8] were detected as 1.09 ns and 0.04, respectively (Figures S29 and 30), which were much larger than those of OF-1. These results could be probably attributed to the restriction of intramolecular rotation in 1 by CB[8].[17] To verify this hypothesis, CB[7], a homologue of CB[8] with a smaller cavity that can encapsulate only one guest in its cavity, was selected as the reference in the control experiments. Indeed, no obvious change could be observed in the presence of 2 equivalents of CB[7], suggesting 1:2 host–guest binding stoichiometry. Furthermore, the ^{1}H NMR signals of protons H_{e-h} displayed a dramatic upfield shift, while those

of protons H_{a-d} in OF-1 showed a slight downfield shift, indicating that bispyridinium segments was mainly located in the cavity of CB[7] (Figure S22). Moreover, the addition of CB[7] gave no apparent bathochromic shift in the UV/Vis spectrum of OF-1, but accompanied by the decreased absorbance at 281 and 396 nm (Figure S21a). The fluorescence emission intensity was slightly enhanced upon addition of 2 equivalents of CB[7], indicating the inferior effect of CB[7] on the restriction of intramolecular rotation in OF-1 as compared to CB[8] (Figure S21 b).

Subsequently, the molecular assembling behaviours and photophysical properties of OF-2 with CB[7] and CB[8] were also investigated. As investigated by the UV/Vis absorption and ^{1}H NMR spectroscopy, the binding stoichiometry between OF-2 and CB[8] was in 1:1 molecular ratio, and the inclusion complexation of OF-2 with CB[7] was quite similar to that with OF-1 (Figures S23 and S25). However, in the case of OF-2⊂CB[8], ^{1}H NMR spectral titrations showed that two antiparallel monocharged bispyridinium moieties were concurrently included in the cavity of CB[8], which was quite different from OF-1⊂CB[8] as a result of steric hindrance of *meta*- substitution in OF-2 (Figure S24). Therefore, no apparent intermolecular CT interaction occurred in the OF-2⊂CB[8] assembly. Nevertheless, 1, 2 and their corresponding supramolecular assemblies with CB[7] and CB[8] also exhibited desired reversible cyclization reaction and cycloreversion reaction upon alternating 254 and >490 nm light irradiation, owing to the classic characteristics of photochromic group of DAE (Figure S12 a–f). In addition, no dramatic change was observed for the photocyclization quantum yield (φ_{o-c}) and cycloreversion quantum yield (φ_{c-o}) of 1 and 2 in the presence of CB[7] or CB[8] (Table S1).

In view of the difference in the molecular structures, assembly modes and UV/Vis absorption spectral characteristics of the assemblies 1⊂CB[8] and 2⊂CB[8], we can predict that only OF-1 may achieve visible light-triggered cyclization in the presence of CB[8], because there was a wide absorption band with high molar absorption coefficient in the OF-1⊂CB[8] assembly ranging from 400 to 500 nm, which was not observed in OF-2⊂CB[8]. Hence, we next employed 420 nm visible light to stimulate OF-1⊂CB[8] assembly in aqueous solution. As shown in Figure 3 a, the absorption maximum of OF-1⊂CB[8] at 282 nm and 396 nm gradually decreased and a new absorption at 620 nm corresponding to its closed-form (CF) state emerged and increased with three isosbestic points at 302, 360, 473 nm, respectively, upon continuous visible-light irradiation at 420 nm (Figure 3 a). Accordingly, the colour of the solution changed from yellow to blue (Figure 3 a, inset). Furthermore, the absorption spectral changes of OF-1⊂CB[8] irradiated at 420 nm largely agreed with that at 254 nm, suggesting that the stimulation with low-energy visible light at 420 nm could also motivate the photocyclization reaction of DAE in 1⊂CB[8]. The ring-closing conversion rate was measured as about 80% by ^{1}H NMR spectroscopic examination on the irradiated sample (Figure S26). Subsequently, the UV/Vis absorption, NMR signals and solution colour could be thoroughly restored to the original states upon >490 nm visible light irradiation, indicative of the complete conversion from CF-1⊂CB[8] to OF-1⊂CB[8] assemblies (Figure 3 a and Figure S26). In contrast, all the other
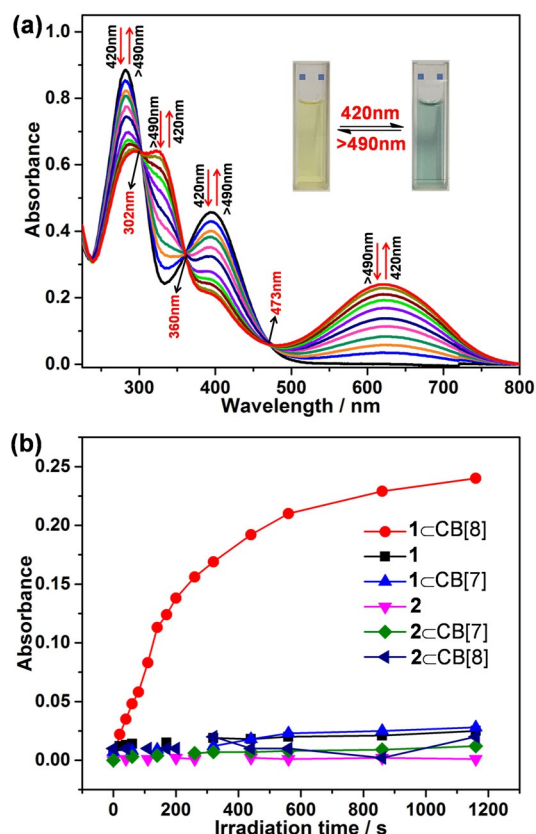
Figure 3. a) UV/Vis absorption spectral changes of OF-1⊂CB[8] upon 420 and >490 nm visible light irradiation, respectively. b) Absorbance variation curves of closed-form of 1⊂CB[8], 1, 1⊂CB[7], 2, 2⊂CB[7], and 2⊂CB[8] over the irradiation time of 420 nm visible light in aqueous solution.

supramolecular assemblies, including 1⊂CB[7], 2⊂CB[7], and 2⊂CB[8], as well as the individual guest 1 or 2, could not achieve such cyclization reaction upon 420 nm visible light irradiation (Figure 3 b and Figure S27), because their OF states have no sufficient absorbance in visible-light region. Moreover, when OF-1⊂CB[8] assembly was irradiated at 420 for 18 minutes, the fluorescence emission intensity was greatly quenched by 86%, which was contributed to the photoisomerization from emissive OF-1⊂CB[8] to nonluminous CF-1⊂CB[8] (Figure 4 a and Figure S28). Subsequently, the quenched fluores-
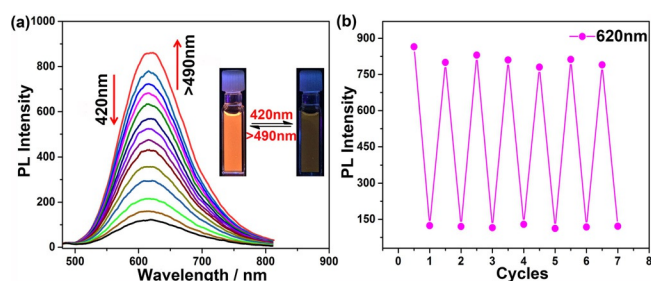

Figure 4. a) Fluorescence spectral changes of assembly 1⊂CB[8] upon 420 and >490 nm light irradiation, respectively. b) Fatigue resistance of visible light-triggered fluorescent switch 1⊂CB[8] ([1] = [CB[8]] = 2×10⁻⁵ M; excitation at 420 nm; slit = 10, 10).

cence of 1⊂CB[8] was completely recovered to its original level upon >490 nm light irradiation. Significantly, this visible light-driven fluorescence switching cycle was repeatable for at least seven times without any obvious fatigue (Figure 4b).

In conclusion, we have synthesized two types of DAE-bridged bispyridinium salts 1 and 2 with subtle structural differences. OF-1 as a molecular rotor could associate with CB[8] to form linear supramolecular assembly OF-1⊂CB[8] driven by the favourable intermolecular CT interaction. More significantly, 1⊂CB[8] could also achieve photocyclization and cycloreversion reactions triggered by visible light (420 and >490 nm, respectively) in both directions, because the intermolecular CT of OF-1 induced by CB[8] could extend the π-conjugation in the whole supramolecular nanosystem and further cause the bathochromic shift of absorption band into visible region. Meanwhile, CB[8] turned on the fluorescence emissive channel of OF-1, which mainly originated from the restriction of intramolecular chemical bond rotation through host–guest complexation, thus giving reversible photophysical behaviour by dual visible-light regulation. Our results will definitely furnish a new strategy for the development of visible light-driven supramolecular fluorescent biomaterials and molecular machines.

Acknowledgements

Conflict of interest

The authors declare no conflict of interest.

[1] P. K. Kundu, D. Samanta, R. Leizrowice, B. Margulis, H. Zhao, M. Börner, T. Udayabhaskararao, D. Manna, R. Klajn, *Nature Chem.* **2015**, *7*, 646.
[2] H. Yamaguchi, Y. Kobayashi, R. Kobayashi, Y. Takashima, A. Hashidzume, A. Harada, *Nature Commun.* **2012**, *3*, 603.
[3] a) S. Kawata, Y. Kawata, *Chem. Rev.* **2000**, *100*, 1777; b) M. Irie, *Chem. Rev.* **2000**, *100*, 1685; c) H. Tian, S. Yang, *Chem. Soc. Rev.* **2004**, *33*, 85.
[4] a) L. Hou, X. Zhang, T. C. Pijper, W. R. Browne, B. L. Feringa, *J. Am. Chem. Soc.* **2014**, *136*, 910; b) G. Liu, X. Xu, Y. Chen, X. Wu, H. Wu, Y. Liu, *Chem. Commun.* **2016**, *52*, 7966.
[5] a) A. C. Whalley, M. L. Steigerwald, X. Guo, C. Nuckolls, *J. Am. Chem. Soc.* **2007**, *129*, 12590; b) C. Jia, A. Migliore, N. Xin, S. Huang, J. Wang, Q. Yang, S. Wang, H. Chen, D. Wang, B. Feng, Z. Liu, G. Zhang, D.-H. Qu, H. Tian, M. A. Ratner, H. Q. Xu, A. Nitzan, X. Guo, *Science* **2016**, *352*, 1443.
[6] a) M. Irie, T. Fukaminato, K. Matsuda, S. Kobatake, *Chem. Rev.* **2014**, *114*, 12174; b) D.-H. Qu, Q.-C. Wang, Q.-W. Zhang, X. Ma, H. Tian, *Chem. Rev.* **2015**, *115*, 7543.
[7] D. Bléger, S. Hecht, *Angew. Chem. Int. Ed.* **2015**, *54*, 11338; *Angew. Chem.* **2015**, *127*, 11494.
[8] T. Fukaminato, T. Hirose, T. Doi, M. Hazama, K. Matsuda, M. Irie, *J. Am. Chem. Soc.* **2014**, *136*, 17145.
[9] a) M. T. Indelli, S. Carli, M. Ghirotti, C. Chiorboli, M. Ravaglia, M. Garavelli, F. Scandola, *J. Am. Chem. Soc.* **2008**, *130*, 7286; b) V. W. W. Yam, C.-C. Ko, N. Zhu, *J. Am. Chem. Soc.* **2004**, *126*, 12734.

[10] J.-C. Boyer, C.-J. Carling, B. D. Gates, N. R. Branda, *J. Am. Chem. Soc.* **2010**, *132*, 15766.

[11] K. Mori, Y. Ishibashi, H. Matsuda, S. Ito, Y. Nagasawa, H. Nakagawa, K. Uchida, S. Yokojima, S. Nakamura, M. Irie, H. Miyasaka, *J. Am. Chem. Soc.* **2011**, *133*, 2621.

[12] M. Herder, M. Utecht, N. Manicke, L. Grubert, M. Pätzel, P. Saalfrank, S. Hecht, *Chem. Sci.* **2013**, *4*, 1028.

[13] S. J. Barrow, S. Kasera, M. J. Rowland, J. d. Barrio, O. A. Scherman, *Chem. Rev.* **2015**, *115*, 12320.

[14] a) J. Zhao, Y.-M. Zhang, H.-L. Sun, X.-Y. Chang, Y. Liu, *Chem. Eur. J.* **2014**, *20*, 15108; b) E.-R. Janeček, J. R. McKee, C. S. Y. Tan, A. Nykänen, M. Kettunen, J. Laine, O. Ikkala, O. A. Scherman, *Angew. Chem. Int. Ed.* **2015**, *54*, 5383; *Angew. Chem.* **2015**, *127*, 5473; c) Y. H. Ko, K. Kim, J.-K. Kang,

H. Chun, J. W. Lee, S. Sakamoto, K. Yamaguchi, J. C. Fettinger, K. Kim, *J. Am. Chem. Soc.* **2004**, *126*, 1932.

[15] W. S. Jeon, E. Kim, Y. H. Ko, I. Hwang, J. W. Lee, S.-Y. Kim, H.-J. Kim, K. Kim, *Angew. Chem. Int. Ed.* **2005**, *44*, 87; *Angew. Chem.* **2005**, *117*, 89.

[16] a) X.-L. Ni, S. Chen, Y. Yang, Z. Tao, *J. Am. Chem. Soc.* **2016**, *138*, 6177; b) G. Ghale, W. M. Nau, *Acc. Chem. Res.* **2014**, *47*, 2150.

[17] G. Liu, Y.-M. Zhang, X. Xu, L. Zhang, Y. Liu, *Adv. Opt. Mater.* **2017**, *5*, 1700149.